Published in final edited form as:
Dev Biol. 2011 January 15; 349(2): 331–341. doi:10.1016/j.ydbio.2010.11.015.

The mouse KRAB zinc-finger protein CHATO is required in embryonic-derived tissues to control yolk sac and placenta morphogenesis

Maho Shibata and **María J. García-García**[1]

[1] Department of Molecular Biology and Genetics, Cornell University, 259 Biotechnology Building, Ithaca, NY 14853

Abstract

Yolk sac and placenta are required to sustain embryonic development in mammals, yet our understanding of the genes and processes that control morphogenesis of these extraembryonic tissues is still limited. The *chato* mutation disrupts ZFP568, a Krüppel-Associated-Box (KRAB) domain Zinc finger protein, and causes a unique set of extraembryonic malformations, including ruffling of the yolk sac membrane, defective extraembryonic mesoderm morphogenesis and vasculogenesis, failure to close the ectoplacental cavity and incomplete placental development. Phenotypic analysis of *chato* embryos indicated that ZFP568 does not control proliferation or differentiation of extraembryonic lineages, but rather regulates the morphogenetic events that shape extraembryonic tissues. Analysis of chimeric embryos showed that *Zfp568* function is required in embryonic-derived lineages, including the extraembryonic mesoderm. Depleting *Zfp568* affects the ability of extraembryonic mesoderm cells to migrate. However, explanted *Zfp568* mutant cells could migrate properly when plated on appropriate extracellular matrix conditions. We show that expression of Fibronectin and Indian Hedgehog are reduced in *chato* mutant yolk sacs. This data suggests that ZFP568 controls the production of secreted factors required to promote morphogenesis of extraembryonic tissues. Our results support previously undescribed roles of the extraembryonic mesoderm in yolk sac morphogenesis and in the closure of the ectoplacental cavity and identify a novel role of ZFP568 in the development of extraembryonic tissues.

Keywords

placenta; yolk sac; chorion; ectoplacental cavity; extraembryonic mesoderm; KRAB-domain protein; mouse

INTRODUCTION

Yolk sac and placenta are extraembryonic tissues that play critical roles in the early development of mammalian species. Although extraembryonic tissues do not contribute to the adult organism, they are critical to sustain embryonic life inside the uterus by providing nourishment and secreting factors that maintain pregnancy (Watson and Cross, 2005). At early embryonic stages, the yolk sac forms a diffusion barrier that mediates the absorption of

Corresponding author: garciamj@cornell.edu; Phone (607)254-4679; Fax (607)255-6249.

nutrients directly from the uterine compartment (Jollie, 1990; Rossant and Tam, 2002). Additionally, the yolk sac functions as the first hematopoietic organ, playing a critical role nourishing embryos once they depend on a circulatory system to deliver nutrients (Ferkowicz and Yoder, 2005; Fraser and Baron, 2009). Once embryonic blood circulation is established, the chorio-allantoic placenta (referred onwards as placenta) becomes essential for embryonic survival, as it mediates the exchange of gases, metabolites and waste products between the maternal and fetal circulatory systems. Placental cell types also secrete hormones that maintain pregnancy and impede immunological rejection of the fetus by the maternal immune system (Watson and Cross, 2005). The importance of extraembryonic tissues is underscored by the embryonic growth restriction and early lethality observed in mouse mutants that disrupt yolk sac and placental development (Argraves and Drake, 2005; Baron, 2003; Watson and Cross, 2005).

There are three critical stages in the morphogenesis of extraembryonic tissues: the early specification of trophectoderm (TE) and visceral endoderm (VE) as extraembryonic lineages separate from the embryonic inner cell mass; the contribution of extraembryonic mesoderm during gastrulation; and the subsequent differentiation and morphogenesis of these cell types to form the mature yolk sac and placenta (Rossant and Tam, 2009). Especially relevant is the emergence of the extraembryonic mesoderm, an embryonic-derived cell type that delaminates from the primitive streak and triggers a profound rearrangement in the other extraembryonic lineages (Inman and Downs, 2007). Starting at embryonic day (E) 6.5, mesoderm cells migrate into the extraembryonic region, displacing TE lineages proximally into the conceptus and originating the exocoelomic and ectoplacental cavities. As the extraembryonic mesoderm thins out to line the exocoelom, it apposes the VE and forms the yolk sac. Additionally, the extraembryonic mesoderm contacts TE lineages and forms the chorion, an extraembryonic membrane essential for placental formation (Rossant and Cross, 2001; Watson and Cross, 2005). Completion of placental morphogenesis also requires the contribution of the allantois, another mesoderm-derived structure that extends and fuses with the chorion, becoming the umbilical cord (Inman and Downs, 2007). Simultaneously, the chorion rises and the ectoplacental cavity collapses, causing the apposition of the chorion with the ectoplacental cone, a pre-requisite for the formation of the labyrinth, the vascularized portion of the placenta where maternal and fetal circulation contact (Inman and Downs, 2007; Watson and Cross, 2005).

The study of mouse mutants has greatly contributed to our understanding of the genes and processes that underlie yolk sac and placenta morphogenesis. More than 90 genes have been described to affect the development of these extraembryonic tissues (for a comprehensive review of mouse mutants with placental phenotypes see Inman and Downs, 2007; Watson and Cross, 2005). Some mutations affect differentiation of extraembryonic cell types: for instance, transcription factors Achaete-Scute complex homolog-2 (ASCL2) and Heart and neural crest derivatives expressed transcript-1 (HAND1) regulate the differentiation of trophoblast giant cells from TE stem cell precursors (El-Hashash et al., 2010; Hu and Cross, 2010). Other mutants affect extraembryonic mesoderm cells or their derivatives, as in the case of mutations in *Brachyury* (*T*) and *Bone morphogenetic protein (Bmp)* signaling, which affect extraembryonic mesoderm morphogenesis and the formation of the allantois (Downs et al., 2004; Inman and Downs, 2006; Rashbass et al., 1991; Tremblay et al., 2001; Winnier et al., 1995). Mouse studies have also highlighted the mutual dependence of TE, VE and extraembryonic mesoderm for morphogenesis of extraembryonic tissues, and have identified signaling molecules that mediate these interactions, including Vascular endothelial growth factor (VEGF), Indian Hedgehog (IHH), Fibroblast growth factor (bFGF), Fibronectin (FN) and Transforming growth factor β (TGFβ) (Bohnsack et al., 2004; Byrd et al., 2002; Damert et al., 2002; Flamme and Risau, 1992; Goumans et al., 1999). Also, TE derived lineages secrete polypeptide hormones that impact proliferation and differentiation of the placenta

(Rossant and Cross, 2001; Watson and Cross, 2005). Studies on mouse mutants have also identified many other genes that control placental morphogenetic processes such as chorioallantoic attachment, labyrinth branching morphogenesis and labyrinth vascularization (reviewed in Inman and Downs, 2007; Watson and Cross, 2005). These include growth factors, adhesion proteins, transmembrane receptors, protein kinases, transcription factors and epigenetic regulators (Bartholin et al., 2008; Inman and Downs, 2007; Papadaki et al., 2007; Rossant and Cross, 2001; Tian et al., 2009; Watson and Cross, 2005).

KRAB Zinc finger proteins represent one of the largest families of transcriptional regulators in mammals, with more than 300 genes (Urrutia, 2003). However, the biological processes controlled by these proteins have been elusive, mostly due to the lack of mouse mutants in individual KRAB-domain proteins. Here we report the characterization of the extraembryonic defects of *chato* mouse mutants. *chato* disrupts ZFP568, a KRAB Zinc finger protein previously described to disrupt mammalian convergent extension (Garcia-Garcia et al., 2008). *chato* mutants display strong extraembryonic defects, including a ruffling of the yolk sac, defective vasculogenesis and incomplete placental morphogenesis. Analysis with markers of different extraembryonic cell types showed proper specification of extraembryonic lineages in *chato* embryos, but morphogenetic cellular and tissue rearrangements were disrupted. *Zfp568* is expressed ubiquitously throughout mid-gestation, but at high levels in TE-derived tissues, including the ectoplacental cone and the extraembryonic ectoderm (Garcia-Garcia et al., 2008). Analysis of chimeric *Zfp568* embryos obtained through tetraploid complementation and through the use of a Cre-responsive *Zfp568* reversible allele indicated that *Zfp568* is required in embryonic-derived tissues for the morphogenesis of both yolk sac and placenta. *chato* mutant yolk sacs contained clumped extraembryonic mesoderm cells, indicating that yolk sac and trophoblast defects in *chato* mutants could be caused by an inability of extraembryonic mesoderm to migrate. We show that *chato* yolk sac explants migrate and behave similar to wild type when plated in appropriate tissue culture conditions, but their migratory ability is diminished in the absence of Fibronectin. Expression of *Fn1* and other factors involved in morphogenesis of extraembryonic tissues is decreased in *chato* mutant embryos. Taken together, these results indicate that *Zfp568* is required in embryonic-derived tissues to provide an environment that supports proper morphogenesis of extraembryonic tissues. Our data attests to the important role of the extraembryonic mesoderm in the morphogenesis of the yolk sac and placenta and defines a requirement of ZFP568 for proper development of these tissues.

MATERIALS AND METHODS

Mouse strains

Extraembryonic phenotypes of $Zfp568^{chato}$ and $Zfp568^{null}$ alleles (Garcia-Garcia et al., 2008) were characterized on C3H/FeJ, CAST/Ei and 129Sv/ImJ. *Meox2Cre* (Tallquist and Soriano, 2000), *Sox2-Cre* (Hayashi et al., 2002) and *ROSA 26* (Friedrich and Soriano, 1991) mice were obtained from Jackson Laboratory. myr-VENUS mice were obtained from Dr. Kat Hadjantonakis (Rhee et al., 2006). The $Zfp568^{rGT\text{-}mutant}$ reversible allele was generated from the German Gene Trap Consortium (GGTC) clone P103E09 (Schnutgen *et al*., 2005). Complete disruption of *Zfp568* splicing in $Zfp568^{rGT\text{-}mutant}$ was confirmed by RT-PCR using primers in *Zfp568* first and second coding exons. For creation of chimeras, $Meox2Cre^{+/-}$; $Zfp568^{+/null}$ or $Sox2Cre^{+/-}$; $Zfp568^{+/null}$ males were crossed to $Zfp568^{rGT\text{-}mutant/+}$ females.

Embryo analysis

Embryos were dissected in 0.4% BSA PBS. Scanning electron microscopy samples were prepared as described (Garcia-Garcia et al., 2008) and imaged with a Hitachi 4500

microscope. *In situ* hybridizations using DIG-labeled RNA probes were conducted as previously described (Garcia-Garcia and Anderson, 2003; Welsh and O'Brien, 2000). Embryos were imaged in methanol, then processed for 16 μm cryosections. Immunohistochemistry was performed as described (Nagy, 2003) on 8 μm cryosections or whole embryos. Antibodies were anti-phospho-histone H3 (1:200; Upstate); anti-VCAM1 (1:250; BD Biosciences), anti-α4 integrin (1:250; Millipore), anti-Laminin (1:50; Sigma-Aldrich), anti-Fibronectin (1:1000 Sigma-Aldrich), anti-E-Cadherin (1:500 Sigma-Aldrich) and anti-rabbit/anti-rat Alexa Fluor 488 (1:200; Molecular Probes). Alexa Fluor 488 Phalloidin (1:20; Molecular Probes) was used for counterstaining. TUNEL was conducted using the ApopTag Kit (Chemicon) as previously described (Garcia-Garcia *et al.*, 2008). Western blot analysis was performed on yolk sacs from E8.5 embryos using standard protocols and anti-Laminin (1:1000; Sigma-Aldrich), anti-Fibronectin (1:1000; Sigma-Aldrich), anti-GAPDH HRP (1:8000; Abcam) and anti-rabbit HRP (1:10000; Jackson ImmunoResearch) antibodies. Intensity of Western blot bands was quantified with ImageJ. Images of mutant embryos and their respective wild type controls are shown at the same magnification. Expression of molecular markers in *chato* mutants of different categories was assayed, but has not been reported unless a modification in the expression pattern was detected. Similarly, analysis of proliferation and apoptosis includes results from *chato* embryos of different classes unless stated. Statistical analysis used two-tailed *t*-tests and the Prism software (GraphPad).

Tetraploid complementation assays

Generation of *Rosa26 lacZ*$^{+}$ *Zfp568*^{chato} and *Zfp568*$^{chato/+}$ ES cell lines, tetraploid complementation experiments and staining for β-galactosidase activity were conducted as described (Nagy, 2003). Similar results were obtained using either of two *Zfp568*^{chato} ES cell lines.

Cell migration assays

Yolk sacs from GFP+ (myr-VENUS; Rhee et al., 2006) wild type embryos and from *chato* mutants were dissected at E8.5 and treated with 0.*25*% trypsin. Trypsinized cells were mixed, then plated onto 5μg/cm^2 Fibronectin-coated chambers. 24 hours after plating, confluent cells were scratched and cultured in media containing 5% FBS. Cell migration was assessed after 16 hours. Individually grown yolk sac explants were performed as described (Nagy, 2003) using Lab-Tek II Chamber Slides (Nunc) coated with 5μg/cm^2 Fibronectin, 5μg/cm^2 Laminin, 0.1% gelatin or without coating. Quantification of migration areas was done at 16 hours using ImageJ. Explants lacking migrating cells at 16 hours (30–60%) were not used to quantify the migratory ability of explants. Differences in explant attachment efficiency between wild type and *chato* mutant embryos, or between different substrate conditions, were not significant.

qRT-PCR

For quantitative reverse transcription PCR analysis of yolk sac samples, RNA was purified from two independent pools of E8.5 wild type and mutant yolk sacs (RNA STAT-60, Tel-Test). SYBR Green real-time PCR was conducted under standard conditions with cDNA prepared using Superscript III First-Strand Synthesis System (Invitrogen). Calculations were conducted using the $2^{-\Delta\Delta CT}$ method (Livak and Schmittgen, 2001) with *Gapdh* as standard. For primer sequences, see Figure S10.

RESULTS

ZFP568 is required for yolk sac morphogenesis

chato is a recessive chemically-induced null mutation in the KRAB domain Zinc Finger protein ZFP568 that disrupts embryo elongation and causes lethality at E9 (Garcia-Garcia et al., 2008). In addition to previously characterized embryonic defects, *chato* mutants display malformations in extraembryonic tissues. In most *chato* embryos (96% n=73), the yolk sac is noticeably ruffled by E8.5 (Figure 1A–B; Garcia-Garcia et al., 2008). These yolk sac bubble-like protrusions were observed in embryos as early as E7.5, although at this stage the yolk sac ruffles were not as large and profuse (Figure 1C–D; Garcia-Garcia et al., 2008). We investigated whether *chato* yolk sac defects originate from abnormalities in the VE or extraembryonic mesoderm, the two cell types that constitute the yolk sac. Analysis of VE markers showed that expression of *α-fetoprotein (Afp)* (Dziadek and Andrews, 1983), *Transthyretin* (*Ttr*) (Barron et al., 1998) and *HNF1 Homeobox B* (*HNF1b*) (Coffinier et al., 1999) was unaffected in *chato* mutants (Figure 1E–H, Figure S1A–D). Likewise, molecular markers of the extraembryonic mesoderm, including *Hand1* (Firulli et al., 1998) and the *Forkhead box F1a* gene (*Foxf1*) (Mahlapuu et al., 2001), were correctly expressed (Figure 1I–L and not shown). We evaluated whether an overgrowth of the VE layer may underlie the yolk sac ruffling in *chato* mutants. To this end, we quantified the number of mitotic cells in sagittal sections using phospho-histone H3 antibodies. The average number of VE mitotic cells in *chato* mutants at E8.5 (6.48±2.38; Figure S1L–M, blue) was slightly smaller than in wild type littermates (7.97±3.18; Figure S1K & S1M, orange), although the difference was not statistically significant (p=0.0655). To evaluate whether the ruffled yolk sac could originate from an excess of VE cells due to increased cell survival, we quantified apoptosis using TUNEL. Consistent with previous reports, we found that wild type yolk sac (Goh et al., 1997) and extraembryonic tissues (Gladdy et al., 2006) have very low levels of apoptosis, and that these levels were similarly low in *chato* mutants (Figure S2). Therefore, our data does not support overproliferation or increased cell survival of the VE as the causes of yolk sac ruffling.

Analysis of *chato* embryo sections revealed abnormalities in the organization of both VE and extraembryonic mesoderm. In *chato* embryos, VE cells were compressed at some areas (Figure 1H, black arrowhead) and detached from the underlying extraembryonic mesoderm at other locations (Figure 1L, red arrowheads; Figure S1B, S1D). These defects were not accompanied by abnormal VE epithelial integrity or polarity, as assessed by analysis of Cadherin 1 (CDH1) and actin localization in *chato* mutants (Figure S1G–J and S1K–L). Integrity and composition of extraembryonic basement membranes were not noticeably changed in *chato* embryos, as judged from immunohistochemistry analysis of Fibronectin and Laminin (Figure S9). Also, expression of receptors for these extracellular components such as α4-Integrin and β1-Integrin was not affected in *chato* mutants (Figure S3 and not shown). Similar to wild type embryos, *chato* mutants contained mesoderm cells lining interiorly the exocoelomic cavity (Figure 1K–L, small arrowheads). However, in *chato* mutants extraembryonic mesoderm cells clumped at the embryonic-extraembryonic junction (Figure 1H, S1, 2D, 2F). Analysis of *Tbx4*, a marker of allantoic mesoderm (Chapman et al., 1996), revealed that posteriorly accumulated cells in *chato* embryos correspond to the allantois, which failed to extend as compared to wild type littermates (Figure 2A–F). In the most severe *chato* embryos, *Tbx4* failed to be expressed (Figure 2E–F). Analysis of markers of vascular and hematopoietic precursors revealed abnormalities in these extraembryonic mesoderm lineages. Immunohistochemistry using Platelet/endothelial cell adhesion molecule-1 (PECAM1) antibodies (Baldwin et al., 1994) showed that in *chato* mutants the vascular endothelial cells are specified, but the extraembryonic vascular plexus failed to extend throughout the yolk sac and remained restricted to the blood island region (Figure 2G–H). Hematopoietic cells were also specified in *chato* mutants (Figure 2I–J, Figure S1E–

F) as highlighted by expression of the hematopoietic marker *βH1globin* (McGrath et al., 2003). However, consistent with the failure of the primitive plexus vasculature to extend in *chato* embryos, they remained confined to the blood island region in *chato* mutants (Figure 2I–J, arrowhead). Altogether, these results indicate that the yolk sac ruffling in *chato* embryos could originate from a loss of adhesiveness between VE and extraembryonic mesoderm, and/or by defective extraembryonic mesoderm morphogenesis.

chato disrupts placental morphogenesis

Morphogenesis of the labyrinth layer of the placenta requires that the allantois grows and makes contact with the chorion (Inman and Downs, 2007; Watson and Cross, 2005). Consistent with the inability of the allantois to extend in *chato* mutants (Figure 2A–F), we found that chorioallantoic attachment was disrupted in all *chato* embryos (n>76), preventing labyrinth formation (Figures 3A–D, S3 and S4). In *chato* mutants containing allantoic buds, adhesion molecules required for chorioallantoic attachment, including Vascular cell adhesion molecule-1 (VCAM1) and its ligand α4-integrin (Gurtner et al., 1995; Kwee et al., 1995; Yang et al., 1995), were localized in allantois and chorionic mesoderm at levels similar to those of wild type littermates (Figure S3). Also, allantoic cell proliferation and cell death were not significantly altered in *chato* mutants (Figure S3M–P). Altogether, these results indicate that *chato* impedes chorioallantoic attachment by disrupting either sustained growth of the allantois or the ability of allantoic cells to migrate.

Analysis of embryonic sections revealed additional malformations in developing placental tissues in *chato* mutants. The majority of *chato* embryos contained an enlarged chorion (92% n=73 Figure 3C–D, Figure S4). Depending on the expansion and arrangement of the chorion we established three *chato* phenotypic groups: In class II *chato* embryos (63%) the chorion expanded laterally in direct contact with the VE (Figure 3C, Figure S4C, S4F), in some cases reaching the embryonic-extraembryonic boundary (Figure 3C, arrowhead). In class III *chato* mutants (29%), the chorion failed to rise and the enlarged chorionic ectoderm formed an expanded ectoplacental cavity (Figure 3D, Figure S4D, S4G). Only 8% of *chato* mutants (class I) contained a normally sized chorion and an ectoplacental cavity that collapsed similar to wild type littermates (Figure 3B).

Expansion of the chorion and failure of the ectoplacental cavity to collapse have not been associated with defects in allantoic growth, as supported by the lack of these defects in mouse mutants that disrupt allantoic extension such as *Smad1* (Lechleider et al., 2001) and *Cdx2* (Chawengsaksophak et al., 2004). To further investigate the role of *Zfp568* in proper morphogenesis of the chorion, we explored whether the expanded chorion in class II and class III *chato* mutants could originate from overproliferation. We assessed the number of phospho-histone H3 positive cells in sagittal section of the chorionic ectoderm at E8.5, when chorioallantoic attachment had just occurred in wild type embryos (Rossant and Cross, 2001) and the chorionic ectoderm cells could still be morphologically discerned from other placental cell types (bracket in Figure 3E). At this stage, we did not observe an overall dramatic difference in the number of phospho-histone H3 positive cells in the chorion of *chato* mutants as compared with wild type littermates (Figure 3E–F). To quantify possible differences, we counted the number of phospho-histone H3 positive cells in the flat chorionic ectoderm of class II *chato* mutants and compared it with the number of TE phospho-histone H3 positive cells closer to the exocoelomic cavity of wild type littermates. Using this method, we found that the chorionic plate of class II *chato* embryos contained only an average of 1.06 more phospho-histone H3 positive cells than those in wild type littermates (wt=4.61 *chato*=5.67; Figure 3G). The fact that this difference is not statistically significant, together with the consideration that our quantification method might slightly underestimate the number of proliferating chorionic ectoderm cells in wild type embryos, suggests that chorion proliferation is not substantially increased in *chato* mutants. As

previously indicated, TUNEL analysis in extraembryonic tissues did not reveal different rates of cell apoptosis between wild type and *chato* littermates (Figure S2), indicating that differences in cell survival do not account for the excess of chorionic ectoderm cells in *chato* embryos.

We next explored whether the expanded chorionic ectoderm in class II and III *chato* mutants could originate from an imbalance amongst different TE lineages. The chorion contains trophoblast stem cells that perdure until the last stages of placental morphogenesis and differentiate to produce ectoplacental cone and trophoblast giant cells (Cross, 2000; Hu and Cross, 2010). Conditions that disrupt the differentiation of trophoblast stem cells lead to an expansion of certain cell types at the expense of others (Guillemot et al., 1994; Luo et al., 1997; Riley et al., 1998). However, analysis of molecular markers characteristic of different placental populations by *in situ* hybridization in whole mount embryos and in sections showed that expression of markers of different placental cell types in *chato* embryos, regardless of their phenotypic class, was similar to that of wild type littermates (Figure S5). The trophoblast giant cell marker *Placental lactogen 1* (*Pl1*); (Linzer and Fisher, 1999) was correctly expressed in *chato* mutants (Figure S5A–D, S5O–P). Likewise, markers expressed in the ectoplacental cone and in precursors of the spongiotrophoblast and labyrinth, including *Ascl2* (Guillemot et al., 1994) and *Trophoblast specific protein alpha* (*Tpbpa*) (Lescisin et al., 1988), were expressed in *chato* embryos in the appropriate location and in a similar number of cells as in wild type littermates (Figure S5E–L). Also, *Glial cells missing homolog 1* (*Gcm1*), a transcription factor expressed in clusters of chorion cells that mark the sites of future labyrinth branching (Basyuk et al., 1999) was expressed in clusters of cells in the chorion of *chato* embryos (Figure S5M–N). These results indicate that *chato* does not influence the differentiation of trophoblast cell types.

Altogether, results from these experiments indicate that ZFP568 does not regulate cell proliferation, cell survival or differentiation of trophoblast lineages. Hypotheses about how the expansion of the chorion might originate in *chato* mutants are provided in the Discussion section.

The severity of trophoblast defects in *chato* embryos correlates with that of yolk sac ruffling and extraembryonic mesoderm defects

We observed that the severity of defects in *chato* trophoblast tissues correlated with that of the yolk sac ruffling and malformations in extraembryonic mesoderm derivatives. In particular, the amount and location of yolk sac ruffles correlated with the extent of chorion expansion. Thus, in *chato* mutants where the chorion expanded to the embryonic-extraembryonic boundary (class II and III), yolk sac protrusions were substantial and concentrated to a small band at this junction (brackets in Figure 3C–D, Figure S5F), while in embryos with a small chorion expansion (some class II) or no chorion expansion (class I), the yolk sac was smoother and the ruffles were distributed throughout a wider band (brackets in Figure 3B, Figure S5J).

Extraembryonic mesoderm defects in *chato* embryos also correlated with the yolk sac and chorion phenotypes. In class I *chato* mutants, clumps of extraembryonic mesoderm were not observed and, even though the vascular plexus was defective, an underdeveloped allantois was present (Figure 2D). However, class II and III *chato* mutants had more severe extraembryonic mesoderm defects such as presence of clumps of extraembryonic mesoderm (Figure 3C) and complete lack of an extended allantoic bud (Figure 2F, Figure 3D).

In contrast to the correlations between the severity of extraembryonic defects in *chato* mutants, we found that neither yolk sac ruffling, chorion expansion, nor extraembryonic mesoderm malformations matched up with the severity of *chato* embryonic phenotypes (not

shown; Garcia-Garcia et al., 2008). Taken together, these observations suggest that defects in yolk sac and trophoblast tissues in *chato* mutants have a common developmental origin, while embryonic malformations likely originate from an independent requirement of ZFP568 in embryonic tissues. Analysis of *Zfp568* expression pattern did not resolve what tissues primarily require ZFP568 function, since *Zfp568* is expressed in all embryonic and extraembryonic tissues at early developmental stages, albeit with higher expression levels in TE cells (Garcia-Garcia et al., 2008; Figure S6).

ZFP568 is required in embryonic-derived tissues to control morphogenesis of embryonic and extraembryonic tissues

To investigate ZFP568 requirements in embryonic and extraembryonic lineages, we analyzed the phenotype of chimeric embryos obtained through tetraploid complementation assays. By aggregating wild type tetraploid embryos with *chato* mutant ES cells, we obtained tetraploid^{wt} ↔ ES cell^{chato} chimeras containing wild type VE and TE (Figure 4A, orange) and *chato* mutant embryonic-derived tissues, including the extraembryonic mesoderm (Figure 4A, blue). We found that tetraploid^{wt} ↔ ES cell^{chato} chimeric embryos (n=12) recapitulated all extraembryonic malformations observed in class II and III *chato* mutant embryos, including yolk sac ruffling (Figure 4B–C, arrowheads; Figure S4F–G), defective extraembryonic and allantoic mesoderm morphogenesis (Figure 4C, Figure S4F–G), expansion of the chorionic ectoderm (Figure 4C, Figure S4F–G) and failure of the chorion to rise and form the placenta (Figure 4C, arrow, Figure S4G). Additionally, tetraploid^{wt} ↔ ES cell^{chato} chimeric embryos displayed embryonic defects similar to *chato* mutants (Garcia-Garcia et al., 2008), including failure to undergo axial rotation and convergent extension defects in lateral plate mesoderm and definitive endoderm (Figure 4D–E). In comparison, control experiments using wild type tetraploid embryos and wild type ES cells, produced embryos without developmental defects (n=13, Figure 4F–I, Figure S4E). Therefore, these experiments demonstrate that wild type ZFP568 function in VE and TE tissues is not sufficient to rescue extraembryonic and embryonic malformations in *chato* mutants and that ZFP568 is required in embryonic-derived tissues to promote both extraembryonic and embryonic morphogenesis.

Restoring *Zfp568* function in embryonic-derived tissues rescues embryonic and extraembryonic defects of *chato* mutants

To further confirm ZFP568 requirement in embryonic-derived tissues, we analyzed the phenotype of chimeric embryos reciprocal to those obtained through tetraploid complementation and thus containing *Zfp568* mutant VE and TE and wild type embryonic-derived tissues (VE+TE^{mutant} ↔ Em+Exm^{wt} chimeras, Figure 5C). To obtain these embryos, we used a *Zfp568* reversible allele in combination with the embryonic-specific Cre lines *Meox2-Cre* (Tallquist and Soriano, 2000) and *Sox2-Cre* (Hayashi et al., 2002). The *Zfp568* reversible allele (*Zfp568*$^{rGT\text{-}mutant}$) contains a genetrap insertion that completely disrupts the activity of *Zfp568* (Figure 5B), but, upon Cre recombinase expression, the orientation of the genetrap cassette can be inverted, restoring partial function to the *Zfp568* locus (*Zfp568*$^{rGT\text{-}restored}$ allele; Figure S7).

To resolve whether restoring *Zfp568* expression in embryonic-derived tissues is sufficient to rescue the extraembryonic and embryonic defects of *chato* mutants, we analyzed the phenotypes of *Meox2-Cre; Zfp568*$^{rGT\text{-}mutant/null}$ and *Sox2-Cre; Zfp568*$^{rGT\text{-}mutant/null}$ embryos. Both allelic combinations generate VE+TE$^{Zfp568\text{-}mutant}$ ↔ Em +Exm$^{Zfp568\text{-partially rescued}}$ chimeras (Figure 5C). The phenotypes of *Meox2-Cre; Zfp568*$^{rGT\text{-}mutant/null}$ and *Sox2-Cre; Zfp568*$^{rGT\text{-}mutant/null}$ chimeric embryos fell into one of the three following categories: some embryos showed all the phenotypic hallmarks of *chato* mutants (Figure 5F); in other embryos, yolk sac and chorion defects were rescued, but

embryos still had *chato*-like defects in embryonic tissues (Figure 5E); finally, some chimeric embryos had a wild-type appearance in both embryonic and extraembryonic tissues (Figure 5D). The lack of rescue in some chimeric embryos (Figure 5E–F) could be due either to incomplete efficiency of the Cre recombinase in all embryonic cells, or to incomplete rescue of ZFP568 function due to the hypomorphic condition of the *Zfp568*$^{rGT\text{-}restored}$ allele (Figure S7). Quantification of embryos showing rescue of yolk sac and embryonic phenotypes showed that a larger percentage of embryos were rescued in experiments using *Sox2-Cre* (Figure 5G–H). This result is consistent with the previously reported higher efficiency of *Sox2-Cre vs. Meox2-Cre* (Hayashi et al., 2002) and confirms that the extent of phenotypic rescue in the chimeras depends, at least partially, on the number of embryonic-derived cells in which ZFP568 function was restored. Regardless of the incomplete Cre efficiency and incomplete restoration of ZFP568 function, the fact that some VE +TE$^{Zfp568\text{-}mutant}$ ↔ Em+Exm$^{Zfp568\text{-partially rescued}}$ chimeras were completely wild type in appearance (Figure 5D, G, H) indicates that relatively small levels of *Zfp568* expression in embryonic-derived tissues can rescue both embryonic and extraembryonic defects. Additionally, the presence of embryonic defects in some VE+TE$^{Zfp568\text{-}mutant}$ ↔ Em +Exm$^{Zfp568\text{-partially rescued}}$ chimeras with rescued yolk sac and placental malformations (Figure 5E) indicates that embryonic defects are not a secondary consequence of the yolk sac and placental malformations in *chato* mutants.

Together with results from the analysis of tetraploid chimeras, these experiments demonstrate that *Zfp568* is not required in the VE or TE for early morphogenesis of the yolk sac, placenta and embryonic tissues. Furthermore, the rescue of extraembryonic, but not embryonic malformations in some VE+TE$^{Zfp568\text{-}mutant}$ ↔ Em+Exm$^{Zfp568\text{-partially rescued}}$ chimeras (Figure 5E) suggests that the requirements for *Zfp568* in extraembryonic mesoderm might be lower, and separate from the requirements of *Zfp568* in embryonic tissues.

chato mutant cells migrate properly in explant assays

Since analysis of chimeric embryos showed that *Zfp568* is required in embryonic-derived tissues (including extraembryonic mesoderm), we sought to test whether extraembryonic defects in *chato* embryos are due to an inability of extraembryonic mesoderm cells to migrate properly. To this end, we compared the migratory ability of wild type and *chato* mutant cells side-by-side in yolk sac explant assays. Yolk sac tissues from GFP-labelled wild type embryos and *chato* mutants were individually trypsinized, then mixed. The resultant cell mixture was then plated onto Fibronectin-coated plates and the migratory behavior of wild type and *chato* mutant cells was evaluated through their ability to populate a scratch as previously described (materials and methods; Figure 6A). If the migratory ability of *chato* mutant cells were hindered, we anticipated that the wound would be preferentially populated by wild type (GFP+) cells. In our experiments, we observed that, at 16 hours after wounding, the scratch had completely healed and contained a similar number of wild type (GFP+) and *chato* mutant (GFP−) cells with mesenchymal morphology that were distributed evenly throughout the wounded area (Figure 6B–C, n=7 assays). We did not detect any abnormality in the morphology of *chato* mutant cells in our tests.

The lack of migratory defects in *chato* mutant explants contrasts with the extraembryonic and embryonic phenotypes we observed in *chato* mutants. As described previously, *chato* embryos contained clumps of extraembryonic mesoderm accumulated in the embryonic-extraembryonic boundary (Figure 2C–F) and extraembryonic mesoderm derivatives fail to properly rearrange to form the vascular plexus (Figure 2G–H). Additionally, *chato* mutants fail to undergo convergent extension (Garcia-Garcia et al., 2008). Since these phenotypes indicate that *chato* regulates cellular rearrangements, we reasoned that *Zfp568* might be required to influence the behavior and/or migration of mesenchymal cells in the context of

the embryo. Cell migration depends on cues laid down in the extracellular environment, such as growth factors, adhesion molecules and chemotactic cues (Ridley et al., 2003). Hence, it is possible that in our explant assays, *chato* mutant cells migrated normally because these cues were provided by either the simultaneous presence of wild type cells or the cell culture conditions. To address this possibility, we tested the migratory ability of wild type and *chato* mutant yolk sac explants when grown separately and under different growth conditions.

We found that different cell culture substrates supported migration from wild type yolk sac explants, although migration was favored when slides were coated with FN (Figure 6D, F, H, J; orange bars in Figure 6L). Previous reports have described similar effects of different extracellular matrix components on cell culture behavior, with particular cell types showing distinct responses for a given protein substrate (Burdsal et al., 1993; Hashimoto et al., 1987; Tzu and Marinkovich, 2008). When plated on FN-coated slides, *chato* yolk sac explants migrated similar to wild type controls (p=0.41; Figure 6D–E, 6L, Figure S8). However, migration from *chato* yolk sacs was significantly reduced when plated on non-coated slides or onto slides coated with inactivated Collagen (gelatin) or Laminin (LAM) (Figure 6F–L, Figure S8). These results indicate that in the absence of FN, *chato* cells do not have the conditions appropriate for cell migration. These results support our previous observation that lack of ZFP568 does not impede cells from migrating in an appropriate environment and suggest that ZFP568 controls the production of specific secreted factors required for cell migration in the context of the embryo.

chato disrupts signaling between VE and extraembryonic mesoderm

Within extraembryonic tissues, a number of molecules secreted to the extracellular environment are required for proper yolk sac morphogenesis. Amongst these, FN1 is known to be produced by extraembryonic mesoderm cells and promote both extraembryonic mesoderm development and VE survival and homeostasis (Bohnsack et al., 2004; Dickson et al., 1995; Goumans et al., 1999; Morikawa and Cserjesi, 2004). Since our explant assays indicated that FN-coating could restore migration from *chato* mutant explants (Figure 6L–M), we investigated whether FN1 was correctly expressed in *chato* embryos. We found that, in *chato* mutants, both FN1 and Laminin A1 (LAMA1)were localized at the basement membranes of extraembryonic and embryonic tissues similar to wild type littermates (Figure S9). However, the levels of FN1 in *chato* yolk sac extracts were 32.2% those of wild type controls as assayed by Western blotting (Figure 7A). Interestingly, the levels of LAMA1 were similar between *chato* and wild type samples (Figure 7B), indicating that *chato* specifically disrupts the production of some, but not all basement membrane components.

In addition to FN1, other secreted factors have been identified to play roles in yolk sac development. VEGF and IHH, are secreted by the VE and promote differentiation and morphogenesis of the vascular system in the adjacent extraembryonic mesoderm layer, where they are bound by receptors exclusively expressed in these cells (Bohnsack et al., 2004; Breier et al., 1992; Farrington et al., 1997; Yamaguchi et al., 1993). Other proteins promoting yolk sac morphogenesis signal within the extraembryonic mesoderm, as is the case of TGFβ1 (Dickson et al., 1995; Larsson et al., 2001; Oshima et al., 1996). To test whether expression of any of these factors or their receptors is regulated by ZFP568, we quantified their levels of expression in yolk sac tissues of wild type and *Zfp568* mutant embryos using qRT-PCR. We found that expression of *Vegfa*, its receptor *Kdr*, and *Tgfβ1* were not significantly different between wild type and *Zfp568* mutant samples (Figure 7C). However, *Zfp568* yolk sac tissues had on average reduced levels of *Ihh* (64%) and *Fn1* transcripts (54%) as compared to wild type littermate controls (Figure 7C). The fact that only some of the factors we tested showed abnormal expression in *chato* mutants excludes the possibility that the *chato* mutation has a general effect on transcription and, hence,

attests of the specificity of these results. Together with the experiments above, these results provide strong evidence that ZFP568 controls the production of specific secreted factors required to promote morphogenesis of extraembryonic tissues.

DISCUSSION

The characterization of *chato* extraembryonic defects demonstrates a role of the KRAB domain Zinc finger protein ZFP568 in the morphogenesis of both yolk sac and placental tissues. In the yolk sac, ZFP568 is required for extraembryonic mesoderm morphogenesis, vasculogenesis, allantois extension and proper organization of the VE layer. ZFP568 loss of function also affects the development of the placenta. In *chato* mutants the allantois fails to extend, disrupting choriallantoic attachment. Furthermore, loss of *Zfp568* causes expansion of chorionic ectoderm and failure of the ectoplacental cavity to collapse, a process required for proper labyrinth formation. Analysis of molecular markers failed to reveal abnormalities in the specification of extraembryonic lineages in *chato* mutants (Figures 1–3). Therefore, our data supports that extraembryonic defects in *chato* embryos arise from abnormalities in the morphogenetic processes that shape these tissues, rather than an imbalance in different extraembryonic cell types.

ZFP568 is expressed ubiquitously throughout embryonic and extraembryonic tissues (Garcia-Garcia et al., 2008). However, the analysis of *chato* chimeric embryos established that ZFP568 is required exclusively in embryonic-derived tissues for early embryo morphogenesis (Figures 4–5). Because extraembryonic mesoderm originates from embryonic lineages during gastrulation (Lu et al., 2001), it is likely that malformations in yolk sac and trophoblast tissues in *chato* mutants arise because of defects in the extraembryonic mesoderm. ZFP568 is also required in embryonic-derived tissues to control morphogenetic processes in the embryo, including convergent extension and axial rotation (Figure 4). Analysis of Cre-induced chimeras using a reversible *Zfp568* allele showed that restoring *Zfp568* function in the embryo and extraembryonic mesoderm, in some cases only rescues defects in yolk sac and trophoblast tissues, but not embryonic morphogenesis (Figure 5). These results support distinct requirements for *Zfp568* in extraembryonic mesoderm and embryonic cells to control morphogenesis of extraembryonic and embryonic tissues, respectively. Together with observations that the severity of embryonic defects do not correlate with that of the extraembryonic malformations, these results support independent roles of ZFP568 in the morphogenesis of embryonic and extraembryonic tissues.

chato affects the secretion of extracellular cues required for proper morphogenesis of extraembryonic tissues

chato mutants have strong defects in extraembryonic mesoderm-derived structures such as the primitive vascular plexus and the allantois (Figure 2). Results from the analysis of chimeric embryos support that vasculogenesis and allantoic malformations in *chato* mutants primarily arise from defects in the extraembryonic mesoderm. Explant assays designed to test the migratory ability of extraembryonic mesoderm cells in *chato* mutants indicate that loss of *Zfp568* does not disrupt the cell machinery required for cell migration (e.g. the cytoskeleton). However, we found that the expression of key molecules required for extraembryonic mesoderm and yolk sac morphogenesis is reduced in *chato* embryos (Figure 7). Fibronectins are well known for their roles in cell adhesion and migration (Glukhova and Thiery, 1993). Specifically, absence of *Fn1* in mouse embryos leads to severe vasculogenesis defects and a separation of the VE from the extraembryonic mesoderm (George et al., 1997). Therefore, the reduced levels of FN1 in *chato* embryos (Figure 7A & C) might be partially responsible for the abnormal vascular plexus, extraembryonic mesoderm migration and VE adhesion defects in *chato* mutants. Noteworthy, *chato* mutant

cells migrate properly when explanted onto FN-coated slides, but their migration is reduced when FN is not provided exogenously (Figure 6, Figure S8).

qRT-PCR experiments also revealed downregulation of *Ihh* levels in *chato* mutants (Figure 7C). *Ihh* is required to sustain yolk sac vasculogenesis (Byrd et al., 2002; Dyer et al., 2001). Hence, lower levels of *Ihh* expression in *chato* embryos may also contribute to the vascular plexus abnormalities in *chato* mutants. Interestingly, *Ihh* is secreted by VE cells (Becker et al., 1997). Since *chato* is required in embryonic-derived tissues, *Ihh* downregulation in *chato* embryos suggests that loss of ZFP568 in the extraembryonic mesoderm indirectly causes malfunctions in the adjacent VE layer. Signaling between the VE and extraembryonic mesoderm is known to be required for proper yolk sac morphogenesis and a number of molecules, including FN1, have been described to mediate these reciprocal interactions (Bohnsack et al., 2004). Therefore, we propose that ZFP568 functions in embryonic-derived tissues to produce factors that signal to adjacent tissues and generate an environment appropriate for extraembryonic mesoderm migration and yolk sac morphogenesis. Comparision of the *chato* phenotype with that of mutants in *Fn1* (George et al., 1997) and *Ihh* (Byrd et al., 2002; Dyer et al., 2001) suggests that the complexity of extraembryonic defects in *chato* embryos is unlikely due to the downregulation of just these factors. We presume that expression of additional molecules required for extraembryonic mesoderm migration and yolk sac morphogenesis might be compromised in *chato* mutants.

chato disrupts morphogenesis of the yolk sac and placenta

chato embryos show severe malformations in non-embryonic-derived tissues, including the yolk sac VE and the chorionic ectoderm. Since *chato* tetraploid chimeras recapitulate the VE ruffling and chorion abnormalities of *chato* mutants, it is likely that these phenotypes are caused by extraembryonic mesoderm defects. It is possible that downregulation of *Fn1*, *Ihh* and/or additional factors in *chato* mutants affects morphogenesis of the VE and chorion. Another possibility is that abnormal morphogenesis of extraembryonic mesoderm in *chato* mutants physically restricts the development of the adjacent VE and TE lineages. Defective genesis (from the primitive streak), migration and/or proliferation of extraembryonic mesoderm might affect the distribution and/or number of cells lining the exocoelomic cavity, which could impair the ability of the VE to extend and in turn cause loss of adhesiveness between these two adjacent layers, originating yolk sac ruffling such as that observed in *chato* embryos.

chato defects in extraembryonic mesoderm also prevent placental morphogenesis. Mouse mutants in which chorioallantoic fusion is blocked retain a flat chorion and display disrupted labyrinth formation (Gurtner et al., 1995; Hunter et al., 1999; Kwee et al., 1995; Yang et al., 1995). Therefore, failure of the allantois to extend and reach the chorion likely prevents labyrinth formation in *chato* mutants (Figure 3F). Additionally, defects in extraembryonic mesoderm migration in *chato* embryos prevent the rising of the chorion and closure of the ectoplacental cavity, processes required for labyrinth formation. Rising of the chorion and closure of the ectoplacental cavity have been described to influence proliferation within the chorionic ectoderm (Uy et al., 2002). Therefore, we hypothesize that delayed or impaired rising of the chorion in *chato* mutants could lead to a subtle increase in chorionic ectoderm proliferation undetectable by phospho-histone H3 analysis, but sustained over time during development. This sustained proliferation could originate the chorionic phenotypes we observed in class II and class III *chato* embryos.

While these observations support that extraembryonic mesoderm defects in *chato* embryos impose a physical constrain in other extraembryonic tissues, mutants that affect extraembryonic mesoderm morphogenesis, such as *T* or *Bmp4* have not been described to cause such severe defects in extraembryonic tissues as *chato* embryos (Rashbass et al., 1991;

Winnier et al., 1995). Therefore, we favor the hypothesis that extraembryonic mesoderm in *chato* mutants both fails to secrete factors that promote morphogenesis and exerts a physical constrain on adjacent tissues.

ZFP568 has overlapping and divergent roles with factors previously described to regulate morphogenesis of extraembryonic tissues

A number of mutants have been identified that affect morphogenesis of extraembryonic tissues. However, *chato* mutants present a unique combination of extraembryonic malformations. As previously indicated, mouse mutants that affect extraembryonic mesoderm morphogenesis (Rashbass et al., 1991; Winnier et al., 1995), allantoic extension (Chawengsaksophak et al., 2004; Lechleider et al., 2001) or chorioallantoic attachment (Mahlapuu et al., 2001; Solloway and Robertson, 1999; Xu et al., 1998), have not been described to cause chorion expansion, failure to close the ectoplacental cavity or as severe yolk sac ruffling as we have observed in *chato* embryos. Amongst other mutants known to disrupt placental morphogenesis (Inman and Downs, 2007; Rossant and Cross, 2001; Watson and Cross, 2005), only mutants in the transcription factors *Hand1* (Firulli et al., 1998; Riley et al., 1998; Scott et al., 1999) and *Erf* (Papadaki et al., 2007) resembled some of the characteristic features of *chato* mutants.

Similar to *chato* embryos, *Hand1* mutants have yolk sac ruffling and vasculogenesis defects, but *Hand1* embryos have an imbalance in the differentiation of TE-derived lineages that causes a reduction in *Pl1*-positive trophoblast giant cells with a concomitant expansion of the spongiotrophoblast population expressing *Acsl2* (Riley et al., 1998), a phenotype that we have not observed in *chato* embryos (Figure S5). Mutants in the ets transcriptional repressor *Erf* also show defects remarkably similar to *chato*, including abnormal vasculogenesis, defective chorioallantoic attachment, failure to close the ectoplacental cavity and an expanded chorion layer (Papadaki et al., 2007). However, *Erf* mutants do not show yolk sac ruffles and, unlike *chato* embryos, loss of *Erf* affects the differentiation of trophoblast stem cells causing a reduction in the number of cells expressing *Tpbpa* and lack of *Gcm1* expression in the chorion at E8.5 (Papadaki et al., 2007). The phenotypic similarities and differences of *chato* embryos with *Hand1* and *Erf* mutants suggest overlapping, as well as divergent roles for these factors on the morphogenesis of extraembryonic tissues. Future studies will help clarify how ZFP568, HAND1 and ERF coordinately and separately control development of the yolk sac and placenta.

CONCLUSIONS

The biological processes controlled by KRAB Zinc finger proteins have been elusive, mostly due to the lack of mouse models disrupting individual KRAB-domain family members. The study of *chato* mutants described here identifies a role of *Zfp568* in the morphogenesis of extraembryonic tissues and defines a primary requirement for *Zfp568* in the extraembryonic mesoderm. Our data supports a requirement for ZFP568 in the production of factors important for cell migration and tissue morphogenesis. The differences between the phenotype of *chato* embryos with that of mouse mutants previously described to affect yolk sac and placenta development suggest that *Zfp568* controls extraembryonic development through distinct molecular mechanisms. Future systems biology approaches will be able to identify the precise targets of ZFP568 ultimately responsible for the morphogenesis of extraembryonic tissues.

RESEARCH HIGHLIGHTS

- the yolk sac in chato mutants has bubble like protrusions

- *chato* disrupts allantoic extension, preventing chorioallantoic attachment
- *chato* causes an expansion of the chorion and failure of the ectoplacental cavity to close
- *Zfp568* is required in embryonic-derived tissues, including extraembryonic mesoderm
- *Zfp568* controls the expression of factors required for morphogenesis of extraembryonic tissues

Supplementary Material

Refer to Web version on PubMed Central for supplementary material.

Acknowledgments

We thank Kathryn Anderson, Joaquim Culi, Juan Modolell, Mark Roberson, John Schimenti, Sol Sotillos, members of the laboratory and anonymous reviewers for helpful discussions and comments on the manuscript; Drs. Ruth Arkell, Kathleen McGrath, Deborah Chapman, James Cross, Kat Hadjantonakis, Janet Rossant and Leif Lundh for mice and reagents; Ke-Yu Deng, personnel at Cornell's Center for Materials Research and CARE for technical help. The conditional genetrap *Zfp568* allele was obtained from the German Gene Trap Consortium (GGTC). This work was supported by Basil O'Connor Starter Scholar Research Award #5-FY06-589 from the March of Dimes Foundation and by NIH grant HD060581.

References

Argraves WS, Drake CJ. Genes critical to vasculogenesis as defined by systematic analysis of vascular defects in knockout mice. Anat Rec A Discov Mol Cell Evol Biol. 2005; 286:875–84. [PubMed: 16114069]

Baldwin HS, Shen HM, Yan HC, DeLisser HM, Chung A, Mickanin C, Trask T, Kirschbaum NE, Newman PJ, Albelda SM, et al. Platelet endothelial cell adhesion molecule-1 (PECAM-1/CD31): alternatively spliced, functionally distinct isoforms expressed during mammalian cardiovascular development. Development. 1994; 120:2539–53. [PubMed: 7956830]

Baron MH. Embryonic origins of mammalian hematopoiesis. Exp Hematol. 2003; 31:1160–9. [PubMed: 14662321]

Barron M, McAllister D, Smith SM, Lough J. Expression of retinol binding protein and transthyretin during early embryogenesis. Dev Dyn. 1998; 212:413–22. [PubMed: 9671945]

Bartholin L, Melhuish TA, Powers SE, Goddard-Leon S, Treilleux I, Sutherland AE, Wotton D. Maternal Tgif is required for vascularization of the embryonic placenta. Dev Biol. 2008; 319:285–97. [PubMed: 18508043]

Basyuk E, Cross JC, Corbin J, Nakayama H, Hunter P, Nait-Oumesmar B, Lazzarini RA. Murine Gcm1 gene is expressed in a subset of placental trophoblast cells. Dev Dyn. 1999; 214:303–11. [PubMed: 10213386]

Becker S, Wang ZJ, Massey H, Arauz A, Labosky P, Hammerschmidt M, St-Jacques B, Bumcrot D, McMahon A, Grabel L. A role for Indian hedgehog in extraembryonic endoderm differentiation in F9 cells and the early mouse embryo. Dev Biol. 1997; 187:298–310. [PubMed: 9242425]

Bohnsack BL, Lai L, Dolle P, Hirschi KK. Signaling hierarchy downstream of retinoic acid that independently regulates vascular remodeling and endothelial cell proliferation. Genes Dev. 2004; 18:1345–58. [PubMed: 15175265]

Breier G, Albrecht U, Sterrer S, Risau W. Expression of vascular endothelial growth factor during embryonic angiogenesis and endothelial cell differentiation. Development. 1992; 114:521–32. [PubMed: 1592003]

Burdsal CA, Damsky CH, Pedersen RA. The role of E-cadherin and integrins in mesoderm differentiation and migration at the mammalian primitive streak. Development. 1993; 118:829–44. [PubMed: 7521282]

Byrd N, Becker S, Maye P, Narasimhaiah R, St-Jacques B, Zhang X, McMahon J, McMahon A, Grabel L. Hedgehog is required for murine yolk sac angiogenesis. Development. 2002; 129:361–72. [PubMed: 11807029]

Chapman DL, Garvey N, Hancock S, Alexiou M, Agulnik SI, Gibson-Brown JJ, Cebra-Thomas J, Bollag RJ, Silver LM, Papaioannou VE. Expression of the T-box family genes, Tbx1-Tbx5, during early mouse development. Dev Dyn. 1996; 206:379–90. [PubMed: 8853987]

Chawengsaksophak K, de Graaff W, Rossant J, Deschamps J, Beck F. Cdx2 is essential for axial elongation in mouse development. Proc Natl Acad Sci U S A. 2004; 101:7641–5. [PubMed: 15136723]

Coffinier C, Thepot D, Babinet C, Yaniv M, Barra J. Essential role for the homeoprotein vHNF1/HNF1beta in visceral endoderm differentiation. Development. 1999; 126:4785–94. [PubMed: 10518495]

Cross JC. Genetic insights into trophoblast differentiation and placental morphogenesis. Semin Cell Dev Biol. 2000; 11:105–13. [PubMed: 10873707]

Damert A, Miquerol L, Gertsenstein M, Risau W, Nagy A. Insufficient VEGFA activity in yolk sac endoderm compromises haematopoietic and endothelial differentiation. Development. 2002; 129:1881–92. [PubMed: 11934854]

Dickson MC, Martin JS, Cousins FM, Kulkarni AB, Karlsson S, Akhurst RJ. Defective haematopoiesis and vasculogenesis in transforming growth factor-beta 1 knock out mice. Development. 1995; 121:1845–54. [PubMed: 7600998]

Downs KM, Hellman ER, McHugh J, Barrickman K, Inman KE. Investigation into a role for the primitive streak in development of the murine allantois. Development. 2004; 131:37–55. [PubMed: 14645124]

Dyer MA, Farrington SM, Mohn D, Munday JR, Baron MH. Indian hedgehog activates hematopoiesis and vasculogenesis and can respecify prospective neurectodermal cell fate in the mouse embryo. Development. 2001; 128:1717–30. [PubMed: 11311154]

Dziadek MA, Andrews GK. Tissue specificity of alpha-fetoprotein messenger RNA expression during mouse embryogenesis. EMBO J. 1983; 2:549–54. [PubMed: 6194986]

El-Hashash AH, Warburton D, Kimber SJ. Genes and signals regulating murine trophoblast cell development. Mech Dev. 2010; 127:1–20. [PubMed: 19755154]

Farrington SM, Belaoussoff M, Baron MH. Winged-helix, Hedgehog and Bmp genes are differentially expressed in distinct cell layers of the murine yolk sac. Mech Dev. 1997; 62:197–211. [PubMed: 9152011]

Ferkowicz MJ, Yoder MC. Blood island formation: longstanding observations and modern interpretations. Exp Hematol. 2005; 33:1041–7. [PubMed: 16140152]

Firulli AB, McFadden DG, Lin Q, Srivastava D, Olson EN. Heart and extra-embryonic mesodermal defects in mouse embryos lacking the bHLH transcription factor Hand1. Nat Genet. 1998; 18:266–70. [PubMed: 9500550]

Flamme I, Risau W. Induction of vasculogenesis and hematopoiesis in vitro. Development. 1992; 116:435–9. [PubMed: 1286617]

Fraser ST, Baron MH. Embryonic fates for extraembryonic lineages: New perspectives. J Cell Biochem. 2009; 107:586–91. [PubMed: 19415688]

Friedrich G, Soriano P. Promoter traps in embryonic stem cells: a genetic screen to identify and mutate developmental genes in mice. Genes Dev. 1991; 5:1513–23. [PubMed: 1653172]

Garcia-Garcia MJ, Anderson KV. Essential role of glycosaminoglycans in Fgf signaling during mouse gastrulation. Cell. 2003; 114:727–37. [PubMed: 14505572]

Garcia-Garcia MJ, Shibata M, Anderson KV. Chato, a KRAB zinc-finger protein, regulates convergent extension in the mouse embryo. Development. 2008; 135:3053–62. [PubMed: 18701545]

George EL, Baldwin HS, Hynes RO. Fibronectins are essential for heart and blood vessel morphogenesis but are dispensable for initial specification of precursor cells. Blood. 1997; 90:3073–81. [PubMed: 9376588]

Gladdy RA, Nutter LM, Kunath T, Danska JS, Guidos CJ. p53-Independent apoptosis disrupts early organogenesis in embryos lacking both ataxia-telangiectasia mutated and Prkdc. Mol Cancer Res. 2006; 4:311–8. [PubMed: 16687486]

Glukhova MA, Thiery JP. Fibronectin and integrins in development. Semin Cancer Biol. 1993; 4:241–9. [PubMed: 8400146]

Goh KL, Yang JT, Hynes RO. Mesodermal defects and cranial neural crest apoptosis in alpha5 integrin-null embryos. Development. 1997; 124:4309–19. [PubMed: 9334279]

Goumans MJ, Zwijsen A, van Rooijen MA, Huylebroeck D, Roelen BA, Mummery CL. Transforming growth factor-beta signalling in extraembryonic mesoderm is required for yolk sac vasculogenesis in mice. Development. 1999; 126:3473–83. [PubMed: 10409495]

Guillemot F, Nagy A, Auerbach A, Rossant J, Joyner AL. Essential role of Mash-2 in extraembryonic development. Nature. 1994; 371:333–6. [PubMed: 8090202]

Gurtner GC, Davis V, Li H, McCoy MJ, Sharpe A, Cybulsky MI. Targeted disruption of the murine VCAM1 gene: essential role of VCAM-1 in chorioallantoic fusion and placentation. Genes Dev. 1995; 9:1–14. [PubMed: 7530222]

Hashimoto K, Fujimoto H, Nakatsuji N. An ECM substratum allows mouse mesodermal cells isolated from the primitive streak to exhibit motility similar to that inside the embryo and reveals a deficiency in the T/T mutant cells. Development. 1987; 100:587–98. [PubMed: 3327671]

Hayashi S, Lewis P, Pevny L, McMahon AP. Efficient gene modulation in mouse epiblast using a Sox2Cre transgenic mouse strain. Mech Dev. 2002; 119(Suppl 1):S97–S101. [PubMed: 14516668]

Hu D, Cross JC. Development and function of trophoblast giant cells in the rodent placenta. Int J Dev Biol. 54:341–54. [PubMed: 19876834]

Hu D, Cross JC. Development and function of trophoblast giant cells in the rodent placenta. Int J Dev Biol. 2010; 54:341–54. [PubMed: 19876834]

Hunter PJ, Swanson BJ, Haendel MA, Lyons GE, Cross JC. Mrj encodes a DnaJ-related co-chaperone that is essential for murine placental development. Development. 1999; 126:1247–58. [PubMed: 10021343]

Inman KE, Downs KM. Brachyury is required for elongation and vasculogenesis in the murine allantois. Development. 2006; 133:2947–59. [PubMed: 16835439]

Inman KE, Downs KM. The murine allantois: emerging paradigms in development of the mammalian umbilical cord and its relation to the fetus. Genesis. 2007; 45:237–58. [PubMed: 17440924]

Jollie WP. Development, morphology, and function of the yolk-sac placenta of laboratory rodents. Teratology. 1990; 41:361–81. [PubMed: 2187257]

Kwee L, Baldwin HS, Shen HM, Stewart CL, Buck C, Buck CA, Labow MA. Defective development of the embryonic and extraembryonic circulatory systems in vascular cell adhesion molecule (VCAM-1) deficient mice. Development. 1995; 121:489–503. [PubMed: 7539357]

Larsson J, Goumans MJ, Sjostrand LJ, van Rooijen MA, Ward D, Leveen P, Xu X, ten Dijke P, Mummery CL, Karlsson S. Abnormal angiogenesis but intact hematopoietic potential in TGF-beta type I receptor-deficient mice. Embo J. 2001; 20:1663–73. [PubMed: 11285230]

Lechleider RJ, Ryan JL, Garrett L, Eng C, Deng C, Wynshaw-Boris A, Roberts AB. Targeted mutagenesis of Smad1 reveals an essential role in chorioallantoic fusion. Dev Biol. 2001; 240:157–67. [PubMed: 11784053]

Lescisin KR, Varmuza S, Rossant J. Isolation and characterization of a novel trophoblast-specific cDNA in the mouse. Genes Dev. 1988; 2:1639–46. [PubMed: 3215514]

Linzer DI, Fisher SJ. The placenta and the prolactin family of hormones: regulation of the physiology of pregnancy. Mol Endocrinol. 1999; 13:837–40. [PubMed: 10379883]

Livak KJ, Schmittgen TD. Analysis of relative gene expression data using real-time quantitative PCR and the 2(−Delta Delta C(T)) Method. Methods. 2001; 25:402–8. [PubMed: 11846609]

Lu CC, Brennan J, Robertson EJ. From fertilization to gastrulation: axis formation in the mouse embryo. Curr Opin Genet Dev. 2001; 11:384–92. [PubMed: 11448624]

Luo J, Sladek R, Bader JA, Matthyssen A, Rossant J, Giguere V. Placental abnormalities in mouse embryos lacking the orphan nuclear receptor ERR-beta. Nature. 1997; 388:778–82. [PubMed: 9285590]

Mahlapuu M, Ormestad M, Enerback S, Carlsson P. The forkhead transcription factor Foxf1 is required for differentiation of extra-embryonic and lateral plate mesoderm. Development. 2001; 128:155–66. [PubMed: 11124112]

McGrath KE, Koniski AD, Malik J, Palis J. Circulation is established in a stepwise pattern in the mammalian embryo. Blood. 2003; 101:1669–76. [PubMed: 12406884]

Meyers EN, Lewandoski M, Martin GR. An Fgf8 mutant allelic series generated by Cre- and Flp-mediated recombination. Nat Genet. 1998; 18:136–41. [PubMed: 9462741]

Morikawa Y, Cserjesi P. Extra-embryonic vasculature development is regulated by the transcription factor HAND1. Development. 2004; 131:2195–204. [PubMed: 15073150]

Nagy, A. Manipulating the mouse embryo: a laboratory manual. Cold Spring Harbor Laboratory Press; Cold Spring Harbor, N.Y: 2003.

Oshima M, Oshima H, Taketo MM. TGF-beta receptor type II deficiency results in defects of yolk sac hematopoiesis and vasculogenesis. Dev Biol. 1996; 179:297–302. [PubMed: 8873772]

Papadaki C, Alexiou M, Cecena G, Verykokakis M, Bilitou A, Cross JC, Oshima RG, Mavrothalassitis G. Transcriptional repressor erf determines extraembryonic ectoderm differentiation. Mol Cell Biol. 2007; 27:5201–13. [PubMed: 17502352]

Rashbass P, Cooke LA, Herrmann BG, Beddington RS. A cell autonomous function of Brachyury in T/T embryonic stem cell chimaeras. Nature. 1991; 353:348–51. [PubMed: 1922339]

Rhee JM, Pirity MK, Lackan CS, Long JZ, Kondoh G, Takeda J, Hadjantonakis AK. In vivo imaging and differential localization of lipid-modified GFP-variant fusions in embryonic stem cells and mice. Genesis. 2006; 44:202–18. [PubMed: 16604528]

Ridley AJ, Schwartz MA, Burridge K, Firtel RA, Ginsberg MH, Borisy G, Parsons JT, Horwitz AR. Cell migration: integrating signals from front to back. Science. 2003; 302:1704–9. [PubMed: 14657486]

Riley P, Anson-Cartwright L, Cross JC. The Hand1 bHLH transcription factor is essential for placentation and cardiac morphogenesis. Nat Genet. 1998; 18:271–5. [PubMed: 9500551]

Rossant J, Cross JC. Placental development: lessons from mouse mutants. Nat Rev Genet. 2001; 2:538–48. [PubMed: 11433360]

Rossant J, Tam PP. Blastocyst lineage formation, early embryonic asymmetries and axis patterning in the mouse. Development. 2009; 136:701–13. [PubMed: 19201946]

Rossant, J.; Tam, PPL. Mouse development: patterning, morphogenesis, and organogenesis. Academic; San Diego, Calif. London: 2002.

Scott IC, Anson-Cartwright L, Riley P, Reda D, Cross JC. The HAND1 basic helix-loop-helix transcription factor regulates trophoblast differentiation via multiple mechanisms. Mol Cell Biol. 1999; 20:530–41. [PubMed: 10611232]

Solloway MJ, Robertson EJ. Early embryonic lethality in Bmp5;Bmp7 double mutant mice suggests functional redundancy within the 60A subgroup. Development. 1999; 126:1753–68. [PubMed: 10079236]

Tallquist MD, Soriano P. Epiblast-restricted Cre expression in MORE mice: a tool to distinguish embryonic vs. extra-embryonic gene function. Genesis. 2000; 26:113–5. [PubMed: 10686601]

Tian Y, Lei L, Cammarano M, Nekrasova T, Minden A. Essential role for the Pak4 protein kinase in extraembryonic tissue development and vessel formation. Mech Dev. 2009; 126:710–20. [PubMed: 19464366]

Tremblay KD, Dunn NR, Robertson EJ. Mouse embryos lacking Smad1 signals display defects in extra-embryonic tissues and germ cell formation. Development. 2001; 128:3609–21. [PubMed: 11566864]

Tzu J, Marinkovich MP. Bridging structure with function: structural, regulatory, and developmental role of laminins. Int J Biochem Cell Biol. 2008; 40:199–214. [PubMed: 17855154]

Urrutia R. KRAB-containing zinc-finger repressor proteins. Genome Biol. 2003; 4:231. [PubMed: 14519192]

Uy GD, Downs KM, Gardner RL. Inhibition of trophoblast stem cell potential in chorionic ectoderm coincides with occlusion of the ectoplacental cavity in the mouse. Development. 2002; 129:3913–24. [PubMed: 12135928]

Watson ED, Cross JC. Development of structures and transport functions in the mouse placenta. Physiology (Bethesda). 2005; 20:180–93. [PubMed: 15888575]

Welsh IC, O'Brien TP. Loss of late primitive streak mesoderm and interruption of left-right morphogenesis in the Ednrb(s-1Acrg) mutant mouse. Dev Biol. 2000; 225:151–68. [PubMed: 10964471]

Winnier G, Blessing M, Labosky PA, Hogan BL. Bone morphogenetic protein-4 is required for mesoderm formation and patterning in the mouse. Genes Dev. 1995; 9:2105–16. [PubMed: 7657163]

Xu X, Weinstein M, Li C, Naski M, Cohen RI, Ornitz DM, Leder P, Deng C. Fibroblast growth factor receptor 2 (FGFR2)-mediated reciprocal regulation loop between FGF8 and FGF10 is essential for limb induction. Development. 1998; 125:753–65. [PubMed: 9435295]

Yamaguchi TP, Dumont DJ, Conlon RA, Breitman ML, Rossant J. flk-1, an flt-related receptor tyrosine kinase is an early marker for endothelial cell precursors. Development. 1993; 118:489–98. [PubMed: 8223275]

Yang JT, Rayburn H, Hynes RO. Cell adhesion events mediated by alpha 4 integrins are essential in placental and cardiac development. Development. 1995; 121:549–60. [PubMed: 7539359]

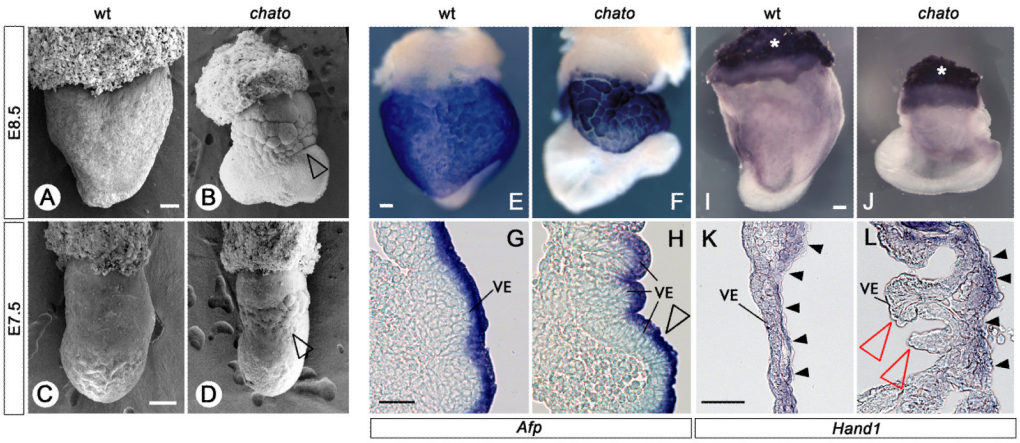

Figure 1. Yolk sac defects in *chato* embryos

(A–D) Scanning electron micrographs of E8.5 (A,B) and E7.5 embryos (C,D). **(E–L)** *In situ* hybridizations in whole mount embryos (E,F, I,J) and yolk sac sections (G,H, K, L) with *Afp* (E–H) and *Hand1* (I–L) probes in E8.5 wild type (E,G, I, K) and *chato* (F, H, J, L) embryos. The *chato* embryos shown in F, H, J and L correspond to the class II category as specified in Figure 3. In this and other figures, the expression of markers in their respective cell types did not change between embryos of different categories unless otherwise noted. Arrowheads in B and D indicate yolk sac ruffles. Arrowhead in H marks compression of VE cells. Red arrowheads in L highlight detachment of VE from extraembryonic mesoderm. Black arrowheads in K, L point to extraembryonic mesoderm cells. Asterisks (I,J) indicate placental expression of *Hand1*. VE, visceral endoderm. Scale bars represent 100μm in A, B, C, D, E and I; and 50μm in G and K. In this and following figures, pictures of wild type and mutant embryos are taken at the same magnification.

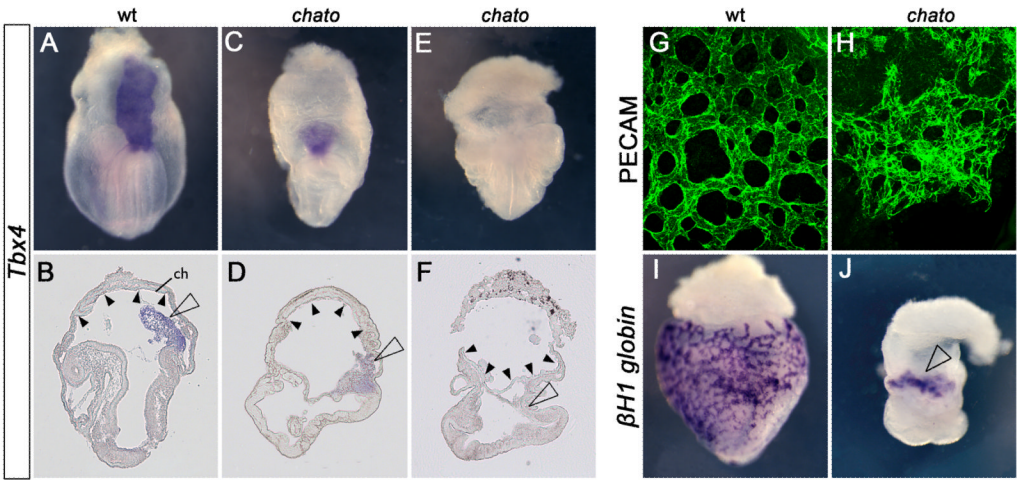

Figure 2. Abnormal extraembryonic mesoderm morphogenesis in *chato* mutants

(A–F) Whole mount *in situ* hybridizations of E8.5 wild type (A,B) and *chato* (C–F) embryos using *Tbx4* probe. (A,C,E) posterior views. (B,D,F) sagittal sections of the corresponding embryos. According to the categories specified in Figure 3, panels D and F are a class I and a class III *chato* mutant, respectively. **(G,H)** Immunohistochemistry with anti-PECAM antibodies in E8.5 wild type (G) and *chato* (H) embryos. Endothelial cells in *chato* mutants are small and formed a collapsed vascular plexus. **(I,J)** *βH1-globin* whole mount *in situ* hybridizations in E8.5 wild type (I) and *chato* (J) embryos. Open arrowheads in B, D, F point to allantoic mesoderm. Arrowhead in J indicates accumulation of blood cells at blood islands. Small arrowheads in B, D and F mark the chorion (ch). Images in G and H were acquired with confocal microscopy using a 40× objective.

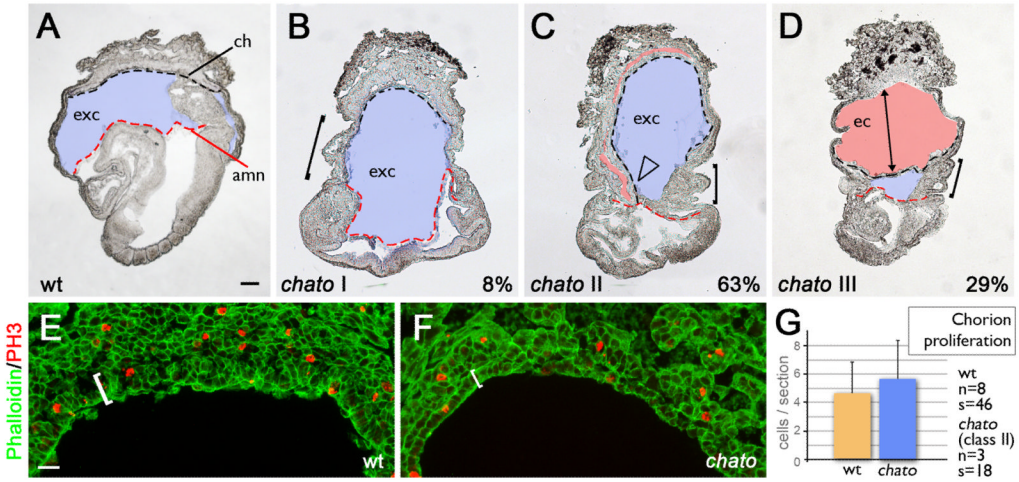

Figure 3. *chato* mutants display chorionic defects

(A–D) Sagittal sections of E8.5 wild type (A) and *chato* (B–D) embryos. Mutants were categorized into class I, II and III based on the severity of chorionic ectoderm expansion. Original pictures of these embryos without labeling signs are shown in Figure S4. **(E–F)** Immunohistochemistry with anti-phospho-histone H3 antibodies (PH3, red) in E8.5 sagittal sections of the chorion in wild type (E) and *chato* (F) embryos counterstained with Phalloidin (green). **(G)** Quantification of the number of PH3 positive cells per section in the chorionic ectoderm of wild type (orange; 4.61±0.33) and *chato* class II (blue; 5.67±0/64) embryos (p=0.1178). Broken black lines mark the chorion (ch). Broken red lines mark the amnion (amn). Exocoelomic cavity (exc) is colored in blue, ectoplacental cavity (ec) is colored in red. Arrowhead in C highlights the expansion of the chorion. Arrow in D points to the enlarged ectoplacental cavity. Bracket in B indicate the relatively smooth yolk sac of class I *chato* mutants. Brackets in C and D indicate yolk sac bubbles concentrated at the embryonic-extraembryonic boundary. Brackets in E and F mark the developing labyrinth in a wild type embryo and the flat chorion of a *chato* mutant, respectively. Error bars indicate s.d.; n=embryos and s=sections quantified. Scale bars represent 100μm in A and 25μm in E.

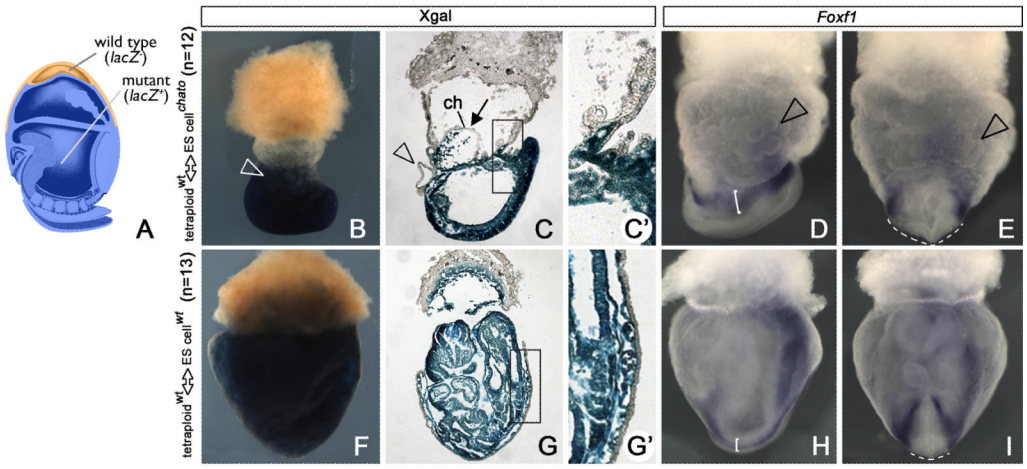

Figure 4. Tetraploid complementation assays

(A) Schematic representation of wild type (orange) and *chato* mutant (blue) cell types in tetraploid^{wt} ↔ ES cell^{chato} chimeric embryos shown in B–E. Tetraploid^{wt} ↔ ES cell^{chato} **(B–E)** and control tetraploid^{wt} ↔ ES cell^{wt} **(F–I)** chimeric embryos were processed for Xgal staining (B–C, F–G) or *Foxf1 in situ* hybridization (D–E, H–I). B, F, D, H; lateral views. E, I; anterior views. C, G; sagittal sections. C′, G′; higher magnifications of boxed areas in C, G. Arrowheads indicate yolk sac ruffles. Arrow in C points to chorion (ch). Brackets in D, H highlight the lateral plate mesoderm. Discontinuous lines in E, I mark the width of the definitive endoderm.

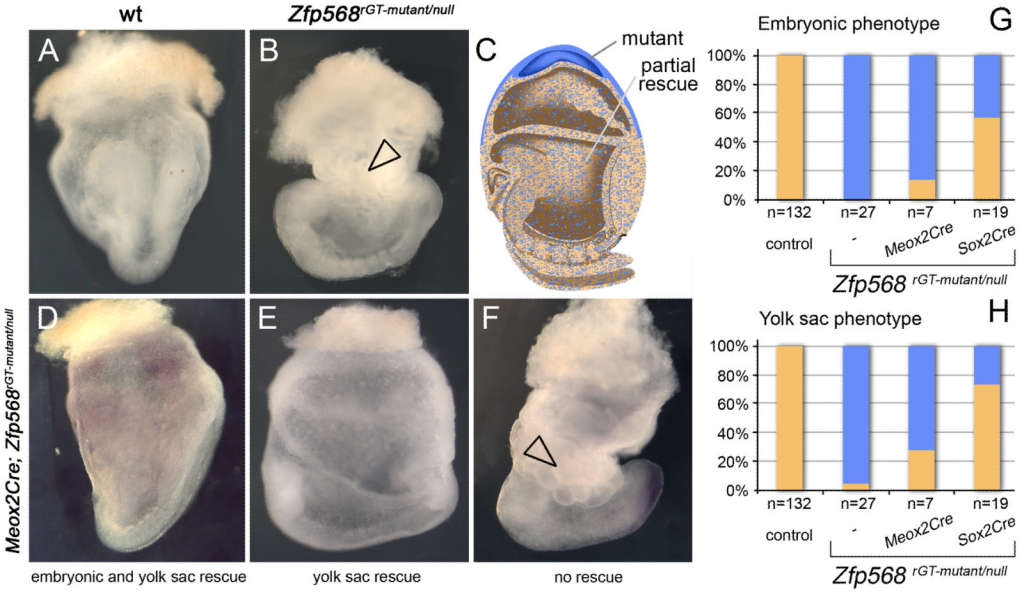

Figure 5. Analysis of chimeras with restored *Zfp568* expression in embryonic-derived tissues

Photographs of E8.5 wild type (A) and *Zfp568*$^{rGT\text{-}mutant/null}$ (B) embryos. **(C)** Schematic representation of the distribution of *Zfp568* mutant cells (blue) and cells with restored *Zfp568* function (orange) in *Meox2Cre; Zfp568* $^{rGT\text{-}mutant/null}$ and *Sox2Cre; Zfp568* $^{rGT\text{-}mutant/null}$ chimeric embryos. **(D–F)** Photographs of *Meox2Cre; Zfp568* $^{rGT\text{-}mutant/null}$ embryos. Blue staining in D and F corresponds to *Zfp568* and *T* expression, respectively. Other embryos were not assayed for expression of these markers. **(G,H)** Quantification of embryos with rescued embryonic (G) and yolk sac phenotypes (H) in *Meox2Cre; Zfp568* $^{rGT\text{-}mutant/null}$ and *Sox2Cre; Zfp568* $^{rGT\text{-}mutant/null}$ chimeras. Trophoblast defects could not be assessed in all chimeras, but severe chorionic defects such as those observed in class II and III *chato* mutants were detected in only 17% (2/12) *Sox2Cre; Zfp568* $^{rGT\text{-}mutant/null}$ embryos, suggesting that trophoblast defects were restored in some chimeras. Orange bars indicate the % embryos in which phenotypes were rescued. Blue bars represent % embryos with *chato*-like phenotypes. Note that yolk sacs were smooth in a small percentage of *Zfp568*$^{rGT\text{-}mutant/null}$ embryos without *Cre* (panel H; orange area in second column from the left; these embryos had a phenotype similar to those shown in panel E). Control embryos include *Sox2Cre/+* and *Meox2Cre/+* embryos. n = embryos quantified. Arrowheads highlight yolk sac ruffles.

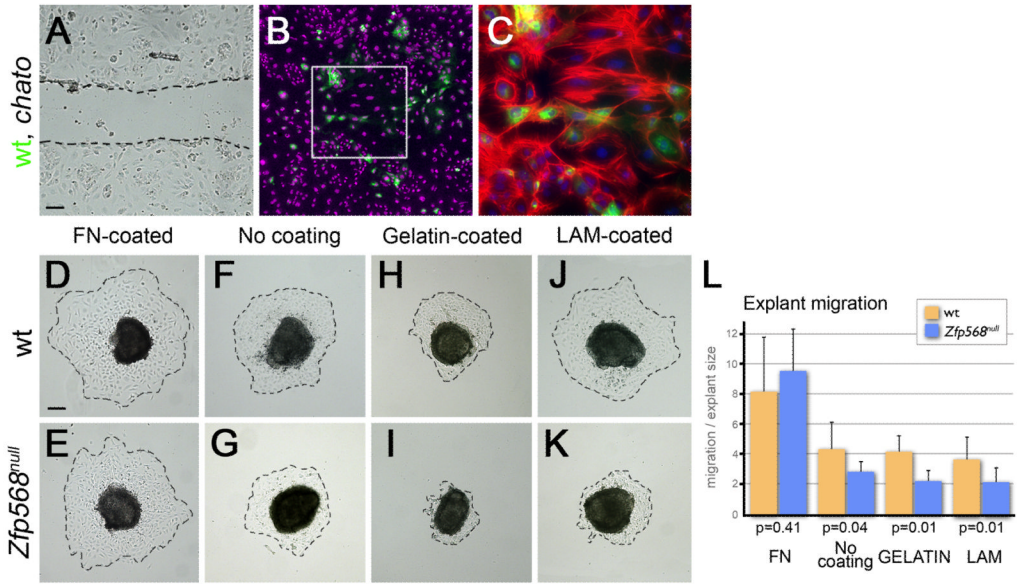

Figure 6. Yolk sac cell migration assays

(A) Bright field image of a scratch made 24 hours after plating a mix of GFP-positive wild type (green in B and C) and *chato* mutant cells from yolk sac explants onto Fibronectin-coated slides. **(B–C)** Phalloidin (red) and DAPI (purple/blue) staining on the same field of cells 16 hours later. C corresponds to the boxed region in B. **(D–K)** Yolk sacs from E7.5 wild type **(D, F, H, J)** and *Zfp568* mutant **(E, G, I, K)** embryos were cut into 2–4 fragments, plated (extraembryonic mesoderm face down) onto chambers coated with Fibronectin (D,E) not coated (F,G), coated with Gelatin (H,I) or Laminin (J,K) and imaged 16 hours afterwards. Images shown are representative examples of each category. For plots of all explants analyzed see Figure S8. **(L)** Quantification of explant migration shown as the area populated by migrating cells from the explant (traced by broken lines in D–K) relative to the size of the explant (dark area in D–K). Broken lines in A indicate edges of scratch. Broken lines in D–K indicate outer edge of migrating cells. Error bars in L represent s.d. between explants. Scale bars represent 100μm in A, D. Orange bars represent wt embryos, blue bars represent *Zfp568*^{null} embryos.

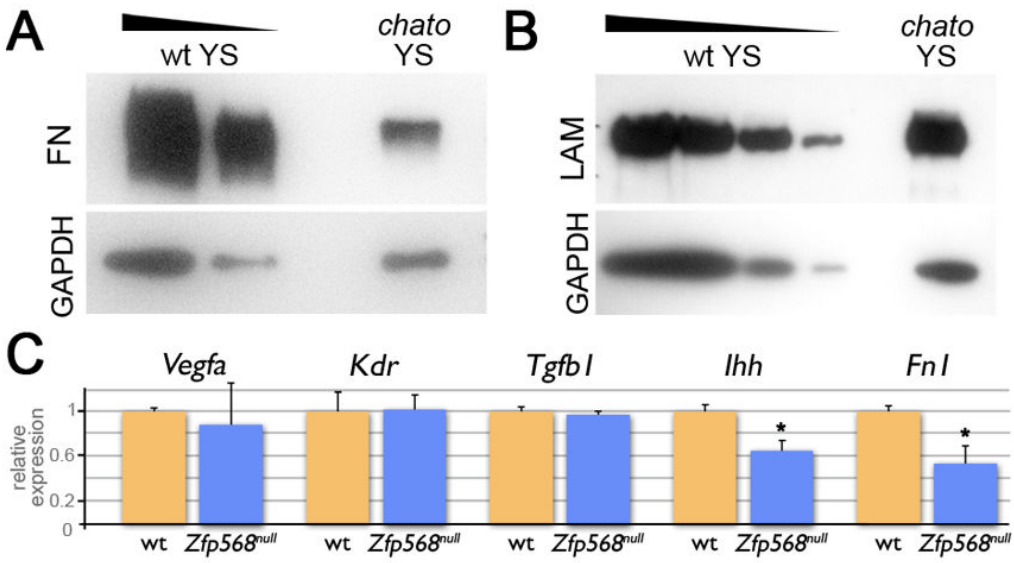

Figure 7. Yolk sac signaling is affected in *chato* mutants

(A–B) Western blots of yolk sac extracts from *chato* and littermate wild type embryos using anti-Fibronectin (A) and anti-Laminin (B) antibodies. GAPDH was used as a loading control. Fibronectin levels were reduced 32.2% (as quantified from 3 different experiments), while Laminin levels were comparable between wild type and *chato* mutant extracts (2 experiments) **(C)** Expression of *Vegfa, Kdr, Tgfb1, Ihh and Fn1* in *chato* (blue) yolk sacs relative to wt (orange) was assessed by qRT-PCR. Error bars represent s.d. between two independent pools of yolk sacs. * indicates $p<0.05$.